Spin physics with antiprotons

ASSIA COLLABORATION

M. Maggiora[2], V. Abazov[1],G. Alexeev[1], M. Alexeev[2], A. Amoroso[2], N. Angelov[1], S. Baginyan[1], F. Balestra[2], V.A. Baranov[1], Yu. Batusov[1], I. Belolaptikov[1], R. Bertini[2], A. Bianconi[3], R. Birsa[10], T. Blokhintseva[1], A. Bonyushkina[1], F. Bradamante[10], A. Bressan[10], M.P. Bussa[2], V. Butenko[1], M. Colantoni[4], M. Corradini[3],S. Dalla Torre[10], A. Demyanov[1], O. Denisov[2], V. Drozdov[1], J. Dupak[8], G. Erusalimtsev[1], L. Fava[4], A. Ferrero[2], L. Ferrero[2], M. Finger, Jr.[1,5], M. Finger [6], V. Frolov[2], R. Garfagnini[2], M. Giorgi[10], O. Gorchakov[1], A. Grasso[2], V. Grebenyuk[1], V. Ivanov[1], A. Kalinin[1], V.A Kalinnikov[1], Yu. Kharzheev[1], Yu. Kisselev[1], N.V. Khomutov[1], A. Kirilov[1], E. Komissarov[1], A. Kotzinian[2], A.S. Korenchenko[1], V.Kovalenko[1], N.P. Kravchuk[1], N.A. Kuchinski[1], E. Lodi Rizzini[3], V. Lyashenko[1], V. Malyshev[1], A. Maggiora[2], A. Martin[10], Yu. Merekov[1], A.S. Moiseenko[1], A. Olchevski[1], V. Panyushkin[1], D. Panzieri[4], G. Piragino[2], G.B. Pontecorvo[1], A. Popov[1], S. Porokhovoy[1], V. Pryanichnikov[1], M. Radici[11], M.P. Rekalo[9], A. Rozhdestvensky[1], N. Russakovich[1], P. Schiavon[10], O. Shevchenko[1], A. Shishkin[1], V.A. Sidorkin[1], N. Skachkov[1], M. Slunecka[6], S. Sosio[2], A. Srnka[8], V. Tchalyshev[1], F. Tessarotto[10], E. Tomasi[7], F. Tosello[2], E.P. Velicheva[1], L. Venturelli[3], L. Vertogradov[1], M. Virius[8], G. Zosi[2] and N. Zurlo[3]

[1]*Dzhelepov Laboratory of Nuclear Problems, JINR, Dubna, Russia*
[2]*Dipartimento di Fisica "A. Avogadro" and INFN - Torino, Italy*
[3]*Università and INFN, Brescia, Italy*
[4]*Universita' del Piemonte Orientale and INFN sez. di Torino, Italy*
[5]*Czech Technical University , Prague, Czech Republic*
[6]*Charles University, Prague, Czech Republic*
[7]*DAPNIA,CEN Saclay, France*
[8]*Inst. of Scientific Instruments Academy of Sciences, Brno, Czech Republic*
[9]*NSC Kharkov Physical Technical Institute, Kharkov, Ukraine*
[10]*University of Trieste and INFN Trieste, Italy*
[11]*INFN sez. Pavia, Italy*

New possibilities arising from the availability at GSI of antiproton beams, possibly polarised, are discussed. The investigation of the nucleon structure can be boosted by accessing in Drell–Yan processes experimental asymmetries related to cross-sections in which the parton distribution functions (PDF) only appear, without any contribution from fragmentation functions; such processes are not affected by the chiral suppression of the transversity function $h_1(x)$. Spin asymmetries in hyperon production and Single Spin Asymmetries are discussed as well, together with further items like electric and magnetic nucleonic form factors and open charm production. Counting rates estimations

are provided for each physical case. The sketch of a possible experimental apparatus is proposed.

Key words: spin physics, antiproton, parton distribution functions, transversity

1 Introduction

The possibility to build a new facility at GSI, a new ring (SIS 300) of the Superconducting Synchrotron with a rigidity of 300 Tm, and to extract from it antiprotons, possibly polarised, provides an excellent tool to investigate the nucleonic structure.

An excellent case to be studied is the di-lepton Drell–Yan production where protons and antiprotons annihilate in the initial state. An important role may be played also by the evaluation of the spin observables in hadron production. I'll concentrate herewith in the relevant topics present in the ASSIA LOI [1].

All these items can be investigated in the framework of the new GSI facility; the key issue is the availability of an antiproton beam, with an energy suitable to investigate the parton distribution functions in a wide range of the Bjorken kinematic variable x. Two different scenarios have been proposed: a slow extraction of the antiprotons from the SIS 300 to a both longitudinally and transversely polarised proton target; an evolution of the GSI HESR toward a collider configuration in which a polarised proton beam would collide with an possibly polarised antiproton beam.

The Drell–Yan interactions are known to be affected by low cross-sections, and yet the investigation of such processes presents several advantages:

1. Due to the non-perturbative vertexes present in the Drell–Yan diagrams (Fig. 1 left), there is no suppression for chirally odd parton distribution functions like transversity.

2. Other kind of hard processes, like semi-inclusive deep-inelastic scattering (SIDIS), can access chirally odd distribution functions, but in the case of Drell–Yan diagrams the parton distribution functions can be directly accessed, while the other processes provide only their convolution with unknown polarised quark fragmentation functions.

3. If we use an antiproton probe, all its constituents can participate to the reaction; if compared with proton-proton or pion-proton scattering, in the Drell–Yan process all the partons taking part to the reaction can be valence quarks, without the need of sea quark.

The selection between the two scenarios must take into account the most relevant parameter, the center of mass energy, that must be high enough to span the desired kinematic region. A complete experiment would require polarised antiprotons, but excellent physics, namely regarding transversity, can be performed also making use of an unpolarised antiproton beam and of a polarised protons.

Also the investigation of the spin dependent cross-sections in exclusive ($p\bar{p} \to \Lambda\bar{\Lambda}$) or semi-inclusive ($p\bar{p} \to \Lambda\bar{\Lambda}X$) strange hadrons production (Fig. 1 right) allows for the extraction of the quark distribution and fragmentation functions. The correlation between the s and $\bar{s}$ quarks can be determined, assuming the spin orientation of the Λ ($\bar{\Lambda}$) given by that of the s ($\bar{s}$) quark, measuring, on an event per event basis, the correlation between the Λ and $\bar{\Lambda}$ polarisations, where the formers can be determined studying the angular distribution of the decay p ($\bar{p}$) in the self analysing weak decay $\Lambda \to p\pi^-$ ($\bar{\Lambda} \to p\pi^-$).

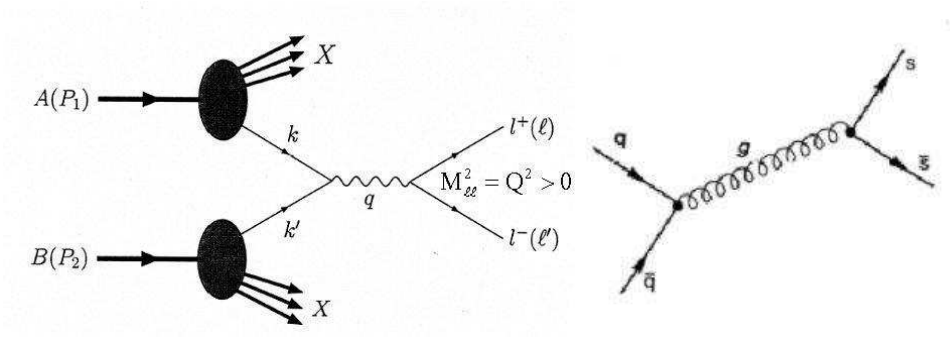

Fig. 1. Left: Drell–Yan dilepton production; right: a quark diagram relevant in hyperons production.

Λ's and $\bar{\Lambda}$'s detection could allow also the investigation of open-charm production in antiproton-proton scattering $\bar{p}p \to \Lambda_c^+ X$.

Spin dependent measurements will also allow to disentangle the electric and magnetic part of the electromagnetic form factors in the exclusive dilepton production from $p\bar{p}$ annihilation.

2 The physics

2.1 Parton distribution functions

At leading twist, in the case of collinear quarks inside the nucleon, or integrating over the transverse momentum of the quarks, the quark structure of the nucleon is completely described by three distribution functions: the unpolarised distribution $f_1(x)$, describing the probability of finding a quark with a fraction x of the longitudinal momentum of the parent hadron, regardless of its spin orientation; the longitudinal polarisation distribution $g_1(x)$, describing the difference between the number density of the quarks with spin parallel and anti-parallel to the spin of a parent longitudinally polarised hadron; and $h_1(x)$ similar to $g_1(x)$, but for transverse polarisation.

If we admit a nonzero quark transverse momentum $\boldsymbol{\kappa}_\perp$ and we do not integrate anymore on it, the nucleon structure is described, at twist two and three, by eight parton distribution functions, among which there are some $\boldsymbol{\kappa}_\perp$-dependent functions. We'll focus later on two $\boldsymbol{\kappa}_\perp$-dependent distributions: $f_{1\mathrm{T}}^\perp(x, \boldsymbol{\kappa}_\perp{}^2)$ and $h_{1\mathrm{T}}^\perp(x, \boldsymbol{\kappa}_\perp{}^2)$,

respectively the distribution functions of an unpolarised quark in a transversely polarised hadron, and of a transversely polarised quark inside an unpolarised parent hadron.

For a complete description of hadron production processes, the fragmentation functions are needed as well; they describe the probability for a quark, in a given polarisation state, to fragment into an hadron carrying some momentum fraction z.

A complete review of the theoretical and experimental aspects relative to parton distribution and fragmentation functions can be found in [2].

2.2 Drell–Yan processes

Let us focus on the production of muon pairs according to the diagram of Fig. 1 left in the process $p\bar{p} \to \mu^+\mu^- X$. Since the virtual photon comes from the quark annihilation vertex, any asymmetry that can be determined depends on the quark distribution functions only functions.

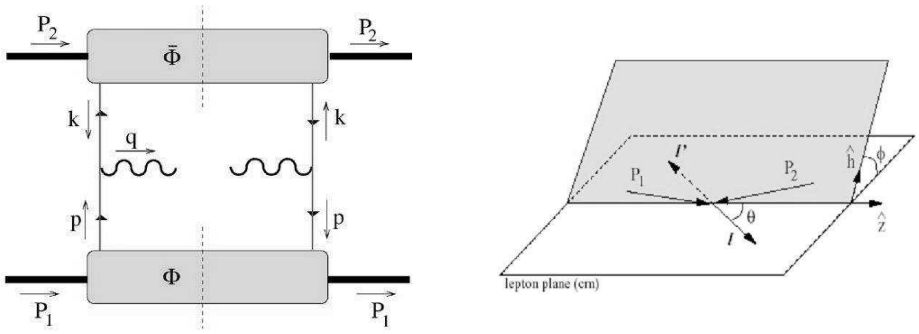

Fig. 2. Left: Hand-bag diagram for a Drell–Yan process; right: the geometry of the Drell–Yan production in the rest frame of the lepton pair [4].

The possibility to access chirally odd parton distribution functions is probably one of the best benefit of the Drell–Yan processes; in such processes in fact the quark lines in the diagram (Fig. 2 left) are uncorrelated, thanks to the two non-perturbative vertexes. Chirally odd amplitudes, and hence transversity $h_1(x)$, can be investigated without the chiral suppression proper of DIS.

We will assume herewith the geometry (Fig. 2 right) and the kinematic variables defined in [4]. The cross-section of the Drell–Yan process $p\bar{p} \to \mu^+\mu^- X$ for a given dimuon mass M, is:

$$\frac{d^2\sigma}{dM^2 dx_F} = \frac{4\pi\alpha^2}{9M^2 s}\frac{1}{(x_1+x_2)}\sum_a e_a^2 \left[f^a(x_1)f^{\bar{a}}(x_2) \; + \; f^{\bar{a}}(x_1)f^a(x_2)\right] \qquad (1)$$

being $x_{1,2} = \frac{M^2}{2P_{1,2}q}$ the fractions of the longitudinal momenta of the incoming hadrons carried by the quark and anti-quarks taking part to the annihilation in the virtual photon; the Feynman variable $x_f = x_1 - x_2$, the ratio of the longitudinal

momentum of the pair to the maximum allowable longitudinal momentum in the colliding hadrons center of mass frame; the parameter $\tau = x_1 x_2 = \frac{M^2}{s}$; and the summing is on the flavour a of the quark ($a = u, d, \mathrm{s}$).

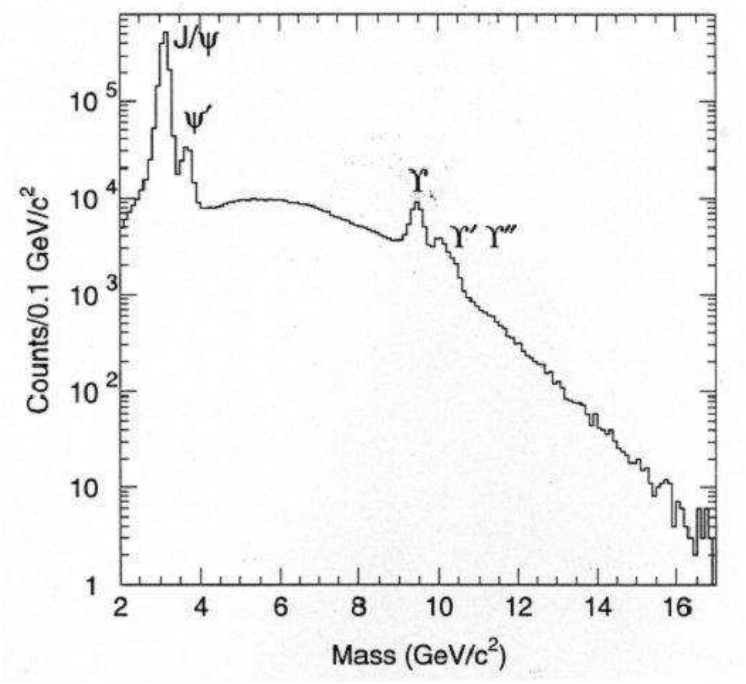

Fig. 3. Combined dimuon mass spectrum from pp and pd collisions (from [5])

.

The scaling properties and the kinematic behaviour of $\mathrm{p\bar{p}} \to \mu^+\mu^- X$ reaction are the same as for the $pp \to \mu^+\mu^- X$; the Drell–Yan cross-section [3, 5] scales as $d^2\sigma/d\sqrt{\tau}dx_F \propto 1/\mathrm{s}$, increasing the statistics in the low beam energy region consistent with the selection of a di-muon mass in the "safe" region, i.e. corresponding to values of M ranging from 4 to $9\,\mathrm{GeV/c^2}$ (Fig. 3). In the "safe" region the dimuon spectrum is essentially continuum without resonance effects from J/Ψ and Υ resonance families to disentangle in the data analysis. For the data arising from the region below the J/Ψ resonance families, perturbative contributions can be important, and the formulæ that we present later on have to be corrected by additional terms; this is the reason why in the ASSIA LOI [1] the safe region only is considered to extract the parton distribution functions. Nevertheless, since there exists arguments in the favour of possibility of studying spin effects in the J/Ψ region [6], and we intend to investigate also the perturbative corrections in the kinematic region below the safe region, data in this kinematic region will be collected as well. The importance of this perturbative effects decreases with increasing s [7].

It is important to investigate the parton distribution functions in the wide region

of x; a wide x_1, x_2 region means asking for the τ parameter to range from 0 to 1. Moreover, to enlarge the statistics, data from the complete safe region should be collected. The upper limit of $9\,\mathrm{GeV/c^2}$ for M defines the highest center of mass energy needed for the complete τ region; the corresponding value for the lowest momentum of the $\bar{\mathrm{p}}$ beam is $40\,\mathrm{GeV/c}$. Also rejecting the events below the J/Ψ peak means to cut the allowed kinematic region. The allowed region in the scatter plot of the two momenta fractions x_1 and x_2, after asking for a dilepton mass above the J/Ψ peak, i.e. above $4\,\mathrm{GeV/c^2}$, depends on the τ value, and thus on center of mass energy s. The hyperbola of Fig. 4 show the τ region selected from the cut on the lowest side of the safe region for different values of s and thus of the beam momentum. The kinematic region that can be accessed making use of antiprotons extracted from SIS 300 at $40\,\mathrm{GeV/c}$ is wider then the region that could be explored by mean of antiprotons colliding on a fixed target in the HESR facility, if the beam energy would be the one foreseen for PANDA [8].

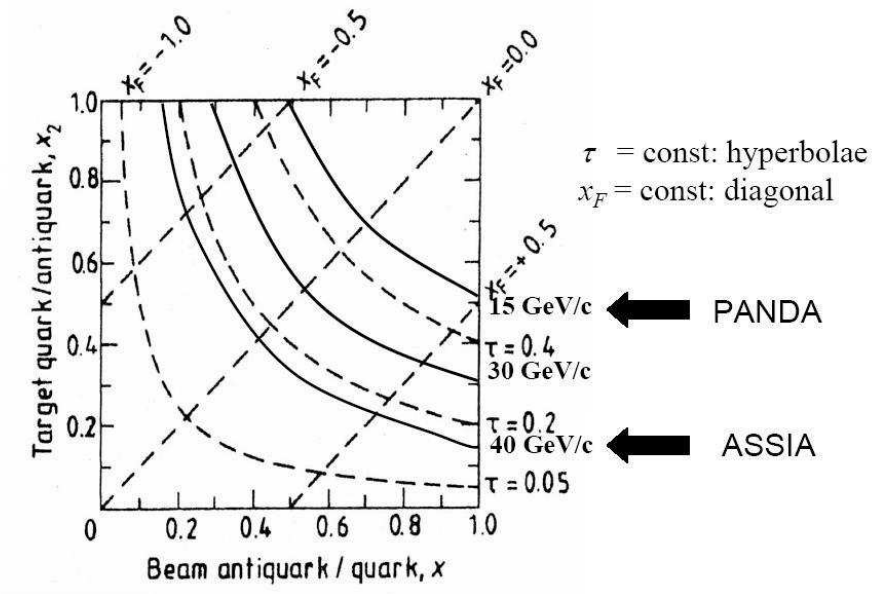

Fig. 4. Allowed kinematic region in x_1 and x_2 for Drell–Yan processes: the regions above the hyperbola correspond to the cut on the dilepton mass $M > 4\,\mathrm{GeV/c^2}$ for three different energies of the beam, the lowest foreseen for PANDA at HESR, the highest proposed by ASSIA for antiprotons extracted from SIS 300.

To ask for the kinetic energy of the $\bar{\mathrm{p}}$ beam the value of $40\,\mathrm{GeV/c}$is a reasonable compromise between the scaling behaviour of the cross-section and the need to cover the wide parton distribution functions range.

The ideal tool would be a beam and a target both polarised either longitudinally

or transversely; in such a case the following asymmetries could be observed:

$$A_{\mathrm{LL}} = \frac{\sum_a e_a^2 g_1^a(x_1) g_1^{\bar{a}}(x_2)}{\sum_a e_a^2 f_1^a(x_1) f_1^{\bar{a}}(x_2)} \tag{2}$$

$$A_{\mathrm{TT}} = \frac{sin^2\,\theta \cos\,2\phi}{1\,+\cos^2\theta} \frac{\sum_a e_a^2 h_1^a(x_1) h_1^{\bar{a}}(x_2)}{\sum_a e_a^2 f_1^a(x_1) f_1^{\bar{a}}(x_2)} \tag{3}$$

$$A_{\mathrm{LT}} = \frac{2\sin\,2\theta \cos\,\phi}{1+\cos^2\theta} \frac{M}{\sqrt{Q^2}} \frac{\sum_a e_a^2 \left(g_1^a(x_1) y g_{\mathrm{T}}^{\bar{a}}(_2) - x h_{\mathrm{L}}^a(x_1) h_1^{\bar{a}}(x_2)\right)}{\sum_a e_a^2 f_1^a(x_1) f_1^{\bar{a}}(x_2)} \tag{4}$$

where the first asymmetry correspond to both a target and a beam longitudinally polarised, the second one to both a target and a beam transversely polarised, and the third asymmetry to the case of one longitudinally polarised and the other transversely polarised. The polar angle θ and the azimuthal angle ϕ are the ones defined in Fig. 2 left and in [4].

It is important to stress that the validity of the formula reported above strongly depends on the assumptions that the center of mass energy and the Q^2 are large enough.

To extract the parton distribution functions these asymmetries have to be compared in a fitting procedure to the experimental asymmetries determined at the same value of x_1 and x_2, after the correction by the factor $1/(P_{\mathrm{b}} \cdot f \cdot P_{\mathrm{T}})$ accounting for the beam polarisation P_{b}, the dilution factor f and the target polarisation P_{T}. For an NH_3 polarised target, as explained in Sec. 3.2, the dilution factor, that is the number of polarised nucleons over the total number of nucleons in the target, would be $f = 1/17 = 0.176$, while a target polarisation $P_{\mathrm{T}} = 0.85$ could be reached.

These asymmetries could be investigated also at RICH, but in the case of a proton-proton scattering, only the sea anti-quark would contribute to the Drell–Yan diagram; moreover, due to the large center of mass energy, $\sqrt{s} \approx 100\,\mathrm{GeV}$, the data would be affected by a strongly reduced cross section and by quite a small allowed kinematic range. The value of the asymmetries itself would be reduced as well, due to the much slower evolution of $h_1(x)$ on Q^2 compared with that of the unpolarised distribution functions [10]; the numerator of the asymmetry ratio would grow slowerly than the denominator, leading thus to suppression of the asymmetries for large values of the center of mass energy.

This would not be the case at GSI, where the center of mass energy would not be so large, and a wide kinematic region could be accessed. If we focus on the double spin asymmetry A_{TT}, the distribution function of a quark of flavour a in the proton can be assumed equal to the distribution function of the anti-quark $\bar{a}$ in the antiproton, since one can be obtained from the other through a charge conjugation. A_{TT} would thus allow a direct access to $h_1(x)$ squared for the valence quark: $h_{1,q_V}(x_1) h_{1,q_V}(x_2)$. It has been shown [11] how this asymmetry is expected to be huge, $\approx 30\,\%$ for a center of mass energy just slightly smaller ($s = 30$–$45\,\mathrm{GeV/c^2}$).

Although the availability of both a polarised beam and a polarised target is the ideal case, spin effects can also be investigated with a polarised target only, or even in a completely unpolarised case.

The angular distribution for dilepton production, for unpolarised beam and target is:

$$\frac{1}{\sigma}\frac{d\sigma}{d\Omega} = \frac{3}{4\pi}\frac{1}{\lambda+3} \times \left(1 + \lambda\cos^2\ \theta + \mu\sin^2\theta\cos\phi + \frac{\nu}{2}\sin^2\theta\cos 2\phi\right) \tag{5}$$

where θ and ϕ are the angular variables above defined. Perturbative QCD calculations at next-to leading order give $\lambda \approx 1$, $\mu \approx 0$, $\nu \approx 0$, confirming the characteristic $\cos^2\theta$ distribution of the decay of a transversely polarised virtual photon, given in the parton model; hence, once accounted for the acceptance, the experimental cross-section should not depend on the azimuthal angle. However fits of experimental data [9, 14] show remarkably large values 30 % of ν at transverse momenta of the lepton pair between 2 and 3 GeV. Recently [12, 13] it has been pointed out that initial state interaction in the unpolarised Drell–Yan process could explain the observed asymmetries and be connected with the quark (anti-quark) T-odd distributions $h_{1q}^{\perp}$ and $h_{1\bar{q}}^{\perp}$.

The measurement, for the $\bar{p}p \to \mu^+\mu^- X$ process, of the $\cos 2\phi$ contribution to the angular distribution of the dimuon pair provides the product $h_1^{\perp}(x_2, \boldsymbol{\kappa}_{\perp}^2)\, \bar{h}_1^{\perp}(x_1, \boldsymbol{\kappa}_{\perp}^{'2})$. This asymmetry can be evaluated also by mean of the PANDA detector, where a polarised target cannot be installed because of the disturbance of the magnetic field of the solenoid; however the maximal antiproton beam energy foreseen for PANDA at HESR limits considerably the reachable kinematic domain for the Bjorken x variable.

In the case of a transversely polarised hydrogen target, the measured asymmetry for the two target spin states depends on the $\sin(\phi + \phi_{S_1})$ term, where ϕ_{S_1} is the azimuthal angle of the target spin in the frame of Fig. 2 right. This term is $\propto h_1(x_2, \boldsymbol{\kappa}_{\perp}^2)\, \bar{h}_1^{\perp}(x_1, \boldsymbol{\kappa}_{\perp}^{'2})$, as shown by [15]:

$$A_{\mathrm{T}} = \mid \boldsymbol{S}_{\perp} \mid \frac{2\,\sin 2\theta \sin(\phi - \phi_{S_1})}{1+\cos^2\theta}\frac{M}{\sqrt{Q^2}} \frac{\sum_a e_a^2 \left[x\left(f_1^{a\perp}(x_1) f_1^{\bar{a}}(x_2) + y h_1^a(x_1) h_1^{\bar{a}\perp}(x_2)\right)\right]}{\sum_a e_a^2 f_1^a(x_1) f_1^{\bar{a}}(x_2)} \tag{6}$$

The ideal scenario would be to combine double spin measurements near the maximum value of the parton distribution functions with the investigation of single spin asymmetries as a function of the Bjorken x to evaluate the x-dependence of the $h_1(X)$ function [16].

With unpolarised antiprotons and polarised protons, the dependence of the quark distribution functions on the quark transverse momentum $\boldsymbol{\kappa}_{\perp}$ could be investigated. In particular, the measurement of the single spin asymmetry (Eq. 6), in the absence of a polarised beam, is a unique tool to probe the $\boldsymbol{\kappa}_{\perp}$ effects. Recently, several papers have stressed the importance of measuring SSA in Drell–Yan processes [17–21]; these measurements allow the determination of new non perturbative spin properties of the proton, like the Sivers function, which describes the azimuthal distribution of quarks in a transversely polarised proton [21].

The study of $\bar{p}^{\uparrow}\, p \to \mu^+\, \mu^-\, X$ processes at GSI offers then unique possibilities.

2.3 Spin asymmetries in hyperon production

It is well known that inclusively produced Λ's, in unpolarised pp interactions show a negative transverse polarisation, that rises with x_F and p_{T} and achieves 40 %. Even higher Λ's polarisation (60 %) was obtained in exclusive reactions like $pp \to p\Lambda K^+$, $pp \to p\Lambda K^+\pi^+\pi^-$ *etc.* [22,23]. This phenomenon has been confirmed many times in extensive set of experiments; yet, its theoretical explanation still remains a persisting problem.

There is a complete correlation between the spin orientations of the Λ and of the $\bar{\Lambda}$. These decays have both a large asymmetry parameter ($\alpha = 0.642$) and branching ratio ($\mathrm{B.R.} = 0.640$).

Different quark-parton models using static SU(6) wave functions were proposed to interpret these polarisation effects by introducing a spin dependence into the partonic fragmentation and recombination processes [24–26]. The Λ polarisation is attributed to some mechanism, based on semi-classical arguments [24, 25] or inspired by QCD [26], by which produced strange quarks acquire a large negative polarisation. Recently a new approach to this problem based on perturbative QCD and its factorisation theorems, and which includes spin and transverse momentum of hadrons in the quark fragmentation, was proposed in [27]. These models are based on different assumptions and are able to explain the main features of the Λ polarisation in unpolarised pp-collisions. To better distinguish between these models more complex phenomena have to be considered.

If the beam or the target is polarised, other observables can be accessed, namely the analysing power, A_{N} [1]), and the depolarisation (sometime referred as spin transfer coefficient), D_{NN}:

$$A_{\mathrm{N}} = \frac{1}{P_{\mathrm{B}} \cos\phi} \frac{N_\uparrow(\phi) - N_\downarrow(\phi)}{N_\uparrow(\phi) + N_\downarrow(\phi)}, \tag{7}$$

$$D_{\mathrm{NN}} = \frac{1}{2P_B \cos\phi} \left[P_{\Lambda\uparrow} \left(1 + P_{\mathrm{B}} A_{\mathrm{N}} \cos(\phi)\right) - P_{\Lambda\downarrow} (1 - P_{\mathrm{B}} A_{\mathrm{N}} \cos(\phi)) \right], \tag{8}$$

where the azimuthal angle ϕ is that between the beam polarisation direction and the normal to Λ production plane.

It is interesting to note that whereas produced Λ polarisation remains large and negative for exclusive and inclusive channels the spin transfer coefficient is negative in low energy (beam momentum 3.67 GeV/c) exclusive production [28], compatible with zero at intermediate energies (beam momentum 13.3 and 18.5 GeV/c) [29] and positive at high energy (beam momentum 200 GeV/c) inclusive reaction [30]. Thus, the measurements at 40 GeV/c can bring an additional information on this phenomenon.

The spin dependence of exclusive annihilation reaction $\bar{p}p \to \bar{\Lambda}\Lambda$ has been considered as relevant to the problem of the intrinsic strangeness component of nucleon [31, 32]. It was demonstrated [33] that the use of a transversely polarised

[1]) A_{N} was studied for π-production also, see Sec. 2.4.

target, in principle, allows the complete determination of the spin structure of the reaction. Corresponding measurements was performed by PS185 Collaboration, see [34] and references therein. Competing models such as t-channel meson exchange model and s-channel constituent quark model reasonably well describing the cross-section of this reaction exist. But both are unable to describe such spin observables as spin transfer from polarised proton to Λ (D_{NN}) and to $\bar{\Lambda}$ (K_{NN}). It is evident that new data on spin transfer and correlation coefficients at higher energies and momentum transfer will be easier interpreted in QCD based approaches and can help a better understanding the spin dynamic of strong interactions.

The semi-inclusive $\bar{p}p \to \bar{\Lambda}\Lambda X$ production is particularly interesting, for which the fundamental Feynman diagram in Fig. 1 right is relevant; the corresponding diagram for this fundamental process would be the one of Fig. 2 left with the virtual photon replaced by a gluon. Therefore the two quarks chiralities are unrelated and there is not a chiral suppression of $h_1(x)$, like in DIS.

Therefore, even with an unpolarised antiproton beam but with a polarised target one can get the spin correlation parameters related both to the parton distributions and to the quark fragmentation functions.

2.4 Single spin asymmetries

Besides the single spin asymmetry defined in Eq. 6 for the Drell–Yan processes, also the investigation of spin effects in hadron production by the mean of the single spin asymmetry:

$$A_{\mathrm{N}} = \frac{d\sigma^{\uparrow} - d\sigma^{\downarrow}}{d\sigma^{\uparrow} + d\sigma^{\downarrow}}\,, \tag{9}$$

would be of relevant importance in the framework of a possible QCD phenomenology. This kind of single spin asymmetry has been measured in $p^{\uparrow}\,p \to \pi\,X$ and $\bar{p}^{\uparrow}\,p \to \pi\,X$ processes, and at large values of x_F ($x_F \gtrsim 0.4$) and moderate values of p_T ($0.7 < p_T < 2.0\,\mathrm{GeV/c}$) have been found by several experiments [29,35,36] to be unexpectedly large. The pion production at large x_F values originates from valence quarks, and according to [37] the A_{N} behaviour (positive for π^+ and negative for π^-) can be explained by Sivers effect, while Collins effect gives negligible contribution; similar values and trends of A_{N} have been found in experiments with center of mass energies ranging from 6.6 up to 200 GeV: this seems to hint at an origin of A_{N} related to fundamental properties of quark distribution and/or fragmentation.

A new experiment with anti-protons scattered off polarised protons, in a new kinematic region, could certainly add information on such spin properties of QCD. Also, A_{N} observed in $\bar{p}\,p^{\uparrow} \to \pi\,X$ processes should be related to A_{N} observed in $\bar{p}^{\uparrow}\,p \to \pi\,X$ reactions, which should be checked.

2.5 Electromagnetic form factors

The study of nucleon electromagnetic form factors is a powerful tool to investigate the nucleon structure; in particular the form factors in the time-like region, which

can be measured through the reactions $\overline{p} + p \leftrightarrow e^+ + e^-$, provide additional informations on the nucleon structure with respect to the ones that can be obtained by the mean of eN-scattering in the space like region. The two regions, space-like and time-like, can be connected analytically through dispersion relations. The form factors data available extend mostly in the space-like region; the data in the time-like region reach higher Q^2, but are less precise; low statistics, imprecise measurements for cross-section (and only for protons and not for neutrons), and no spin effects in the time-like region data are investigated.

The reaction $\bar{p}p \to \mu^+\mu^-$ with polarised p ($\bar{p}$) can be an alternative way to study form factors in the time-like region measuring both the angular distributions of the differential cross-sections and of the analysing power. The angular dependence of the differential cross section for $\overline{p} + p \to \mu^+ + \mu^-$ can be expressed as a function of the angular asymmetry $\mathcal{R}$:

$$\frac{d\sigma}{d(\cos\theta)} = \sigma_0 \left[1 + \mathcal{R}\cos^2\theta\right], \ \mathcal{R} = \frac{\tau|G_M|^2 - |G_E|^2}{\tau|G_M|^2 + |G_E|^2} \tag{10}$$

being $\sigma_0 = \sigma_{\theta=\pi/2}$.

Theoretical models provide for these quantities predictions very sensitive on the different underlying assumptions on the s-dependence of the form factors. Moreover polarisation effects are particularly interesting, since a transverse polarisation P_{T} (of the proton or of the antiproton) results in a nonzero analysing power:

$$\mathcal{A} = \frac{\sin 2\theta Im G_E^* G_M}{D\sqrt{\tau}}, \ D = |G_M|^2(1 + \cos^2\theta) + \frac{1}{\tau}|G_E|^2 \sin^2\theta \tag{11}$$

$$\frac{d\sigma}{d\Omega}(P_{\mathrm{T}}) = \left(\frac{d\sigma}{d\Omega}\right)_0 [1 + \mathcal{A}P_{\mathrm{T}}] \tag{12}$$

The τ-dependence of $\mathcal{A}$ is very sensitive to existing models of the nucleon form factors, which reproduce equally well the data in the space-like region.

Therefore, a precise measurement, either with a polarised antiproton beam or with an unpolarised antiproton beam on polarised protons, would be very interesting in order to achieve a global interpretation of the four nucleon form factors, electric and magnetic, for proton and neutron, both in the space-like and in the time-like region. The angular distribution of the produced leptons for the channels $\bar{p}p \to l^+l^-$ allows for the separation of the electric and magnetic form factors, since the asymmetry $\mathcal{R}$ is sensitive to the relative value of G_M and G_E. Moreover, an experimental proof of a large relative phase of proton magnetic and electric form factors at relatively large momentum transfers in the time-like region would be a strong indication of a different behaviour of these form factors.

2.6 Open charm

Very recently the possibility to use the antiproton beam for open charm production (Fig. 5) has been suggested [38]. In this process both gg and $q\bar{q}$ fusion play an essential role in different kinematic regions and could be used to probe the internal

structure of the nucleon. For both, the antiproton beam is an ideal probe. This study can be pursued detecting, for example, the $\bar{p}p \to \Lambda_c^+ X$ production, where the $\Lambda_c^+ \to \Lambda\,\pi^+$ weak decay and the $\Lambda_c^+ \to \Lambda\,e^+\,\nu_c$ semileptonic decay can be used to infer the c polarisation. The asymmetry parameters for these decays are huge but the branching ratios small so that the feasibility of this option has to be worked out with simulations. It looks very attractive as no data exist in the $s \approx 80$–$90\,\mathrm{GeV}^2$ region.

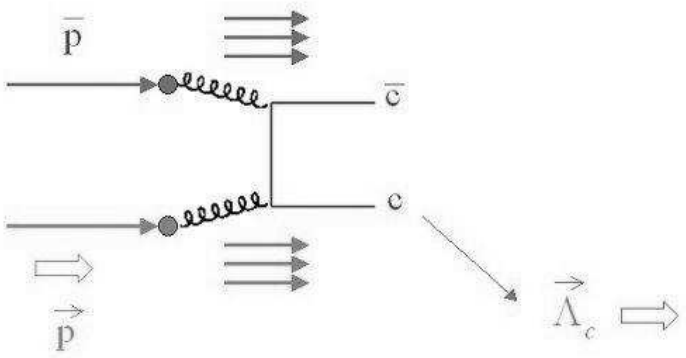

Fig. 5. Open charm production with antiproton beams.

3 Experimental set-up

3.1 Beam and target

The antiproton beam energy foreseen at HESR is 15 GeV/c, with a luminosity, in the case of the PANDA pellet target, of $\leq 2 \times 10^{32}\,\mathrm{cm}^{-2}\,\mathrm{s}^{-1}$ and a momentum spread lower than $\pm 1 \times 10^{-4}$; these excellent performances do not fit with the experimental program we propose, that requires a minimal energy of 40 GeV and a limited momentum resolution. Moreover the present design of the PANDA detector [8] is not compatible with a polarised target.

A different solution could then be foreseen, among the two described in details herewith.

A first possibility would be an antiproton beam of energy ≥ 40 GeV/c extracted from SIS 300 scattering on a polarised target. The expected momentum spread of such a beam should be about $\pm 2 \times 10^{-4}$, that is largely enough for the proposed measurements.

Assuming for the extraction the whole foreseen antiproton production accumulation rate of $7 \times 10^{10}\,\bar{p}$/h, and injection and extraction efficiencies always larger than 0.90, the expected beam intensity on the target is of about $1.5 \times 10^7\,\bar{p} \cdot \mathrm{s}^{-1}$. The target could be similar to the one of the COMPASS apparatus at CERN [39], where two cells with opposite polarisation are put one downstream of the other,

a solution that allows for the minimisation of the systematic errors in asymmetry measurements. In the case of a NH_3 target $15\,g/cm^2$ thick, with a dilution factor $f = 1/17 = 0.176$ and a polarisation $P_T = 0.85$, the expected luminosity is:

$$\mathcal{L} = \frac{3}{17} \times 15 \times 6 \cdot 10^{23} \times 1.5 \cdot 10^{7} = 2.25 \cdot 10^{31}\,\mathrm{cm}^{-2}\,\mathrm{s}^{-1} \tag{13}$$

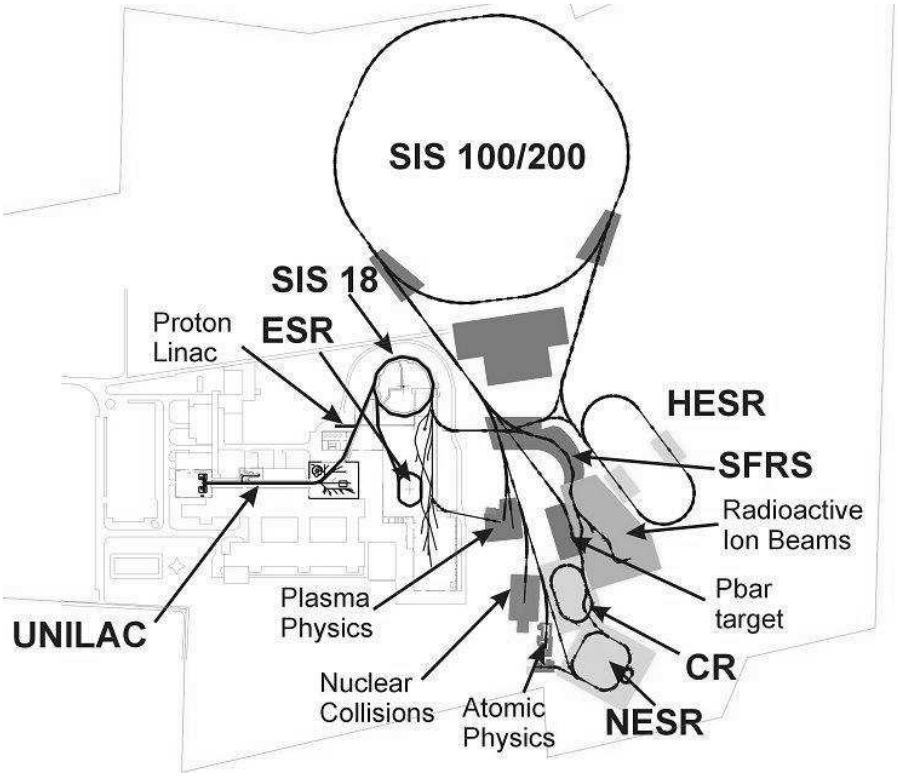

Fig. 6. The new facility layout at GSI; SIS 300 would be an upgrade of the already foreseen SIS 100/200 synchrotron.

The generation of a 40 GeV/c antiproton beam would require the following additional construction or modification items to the presently proposed configuration scheme (Fig. 6) of the new International Accelerator Facility in GSI:

1. extraction of the accelerated antiproton beam from SIS 100 into SIS 300, requiring a transition system to be designed and built; or alternatively an injection scheme from the CR into the SIS 300;

2. a slow extraction system from SIS 300 into a more powerful extraction beamline able to handle momenta larger than 40 GeV/c;

3. a cave housing the experimental setup as proposed which can handle the expected radiation doses (with $\approx 2 \times 10^7\ \bar{p} \cdot \mathrm{s}^{-1}$).

With this scheme, and provided that different spin orientations were available for the polarised target like in the COMPASS set-up [39], both longitudinal and transverse asymmetries could be measured. In addition, if a transversely polarised antiproton beam could be produced and extracted from SIS 300, a unique tool for the study of the nucleon structure would be available.

An alternative solution, proposed by Hans Gutbrod [40], could be to imagine the HESR as a collider with both a polarised proton and antiproton beams interacting with a luminosity comparable to that reachable with an external target; the longitudinal size of the antiproton-proton colliding region should not be larger than few millimetres. If such a luminosity could be reached, the advantage of such a solution would be that thre will be no loss of accuracy due to diluition factor, making the asymmetries measurement more precise for the same number of events collected. The required CM energy $\sqrt{s} \approx 30\,\mathrm{GeV}$ for the proposed program could be easily reached with the present foreseen performances of HESR (15 GeV/c). In addition the higher CM energies available would allow new physics opportunities.

A polarised proton beam of up to 15 GeV/c would require a polarised proton source and an acceleration scheme preserving the polarisation. No new beam line needs to be built and no additional extraction needs to be included into the acceleration system. The lattice of the HESR would have to allow an interaction region of both beams.

The key issues of these two proposals is the luminosity.

3.2 Detector concept

The proposed detector concept (Fig. 7) is inspired from the Large Angle Spectrometer, that is the first part of the COMPASS spectrometer [39]. Such a detector concept would be compatible with an extraction scheme of the antiprotons from SIS 300; if the HESR collider mode should become available, a different set-up, not discussed herewith, should be foreseen.

The Large Angle Spectrometer consists of a large dipole magnet SM1 (a window frame magnet with an aperture of 2.0×1.6, a depth of about 1 m, providing a field integral of about 1 Tm) and tracking detectors of different types, chosen in such a way that they can sustain the beam rate ($1.5 \times 10^7\ \bar{p}$/s) and provide the hits position with such a precision to guarantee the needed resolution for the position of the vertexes of the decaying particles (Λ and $\bar{\Lambda}$) and for the widths of the corresponding peaks in the invariant mass spectra. To reach these goals and also to minimise the overall cost of the apparatus, detectors of smaller size but with thinner resolution and accepting higher rates have been chosen to detect the hits nearer to the beam trajectory. These detectors are GEM and MICROMEGAS, that provide spatial resolutions with $\sigma \leq 70\,\mu$. To detect hits at larger distances from beam trajectories MWPC and STRAW tubes are used that provide spatial resolutions of the order of the millimetre. These last detectors have a dead zone in their central part, that

is nearer to the beam trajectories and covered by the GEM and MICROMEGAS detectors.

With this setup a mass resolution ($\sigma \approx 2.5\,\mathrm{MeV/c^2}$) can be obtained for the Λ ($\bar{\Lambda}$). The expected spatial resolution on the position of the decay vertexes of the Λ ($\bar{\Lambda}$) goes from $\approx 1\,\mathrm{cm}$, for very small angles with the beam trajectories, to a couple of mm for larger angles. This spatial resolution is large enough to base the Λ ($\bar{\Lambda}$) identification on the requirement that these vertexes are outside the target.

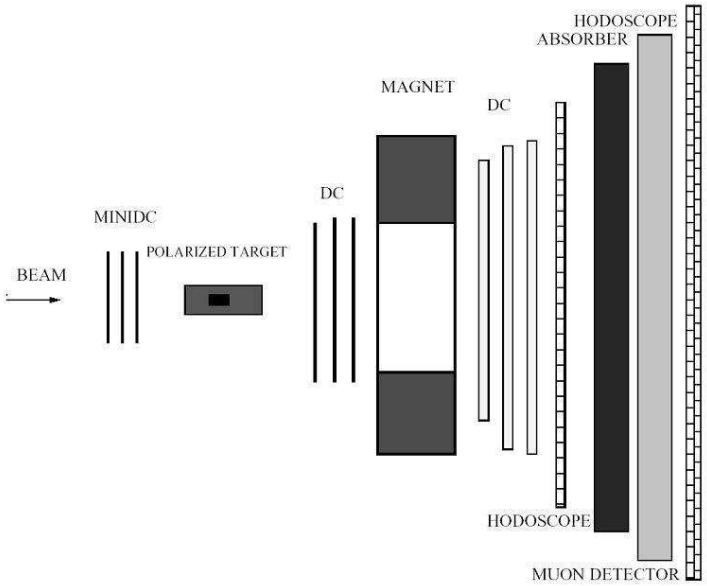

Fig. 7. Sketch of the apparatus. MiniDC stay for such detectors of drift type like GEM's and μMEGAs in COMPASS. DC Stay for a combination of small drift type detectors with high spatial resolution with larger detector with a dead central area.

Trigger is provided by scintillating hodoscopes, asking for a multiplicity greater then 2; muon detection is performed by the mean of sandwiches of iron plates, IAROCCI tubes and scintillator slabs, already present in the COMPASS apparatus.

A vacuum pipe of growing cross-section would catch the beam up to the beam dump to minimise the background related to the interactions of the beam after the target.

3.3 Counting rates

Since the Drell–Yan channel $\bar{p}p \to \mu^+\mu^- X$ is affected by a low cross section, and the hyperon production channel $\bar{p} + p \to \bar{\Lambda} + \Lambda + X$ is affected by strong limits in acceptance, the expected counting rates for these two reactions will be considered

as the limit cases; the case of the proton time like form factors will be discussed later on. An intensity of the antiproton extracted beam at the polarised target of $1.5 \times 10^7\,\bar{p}\cdot\,\mathrm{s}^{-1}$ is assumed, while the expected luminosity is the one of Eq. 13.

The expected cross section for the $\bar{p}p \to \mu^+\mu^- X$ reaction, integrated over positive x_F and all transverse momenta, is about 0.3 nb at 40 GeV/c; it can be extracted scaling as 1/s the data acquired [9] for $\mathrm{p\bar{p}} \to \mu^+\mu^- X$ at 125 GeV/cfor dimuon masses ranging between 4 and 9 $\mathrm{GeV/c^2}$. The expected counting rate is then:

$$\boldsymbol{\mathcal{R}} = 2.25 \cdot 10^{31} \times 3 \cdot 10^{-34} \times A = 6.75 \cdot 10^{-3} \times A \cong 3 \cdot 10^{-3}\,\mathrm{ev.\,s^{-1}} \qquad (14)$$

for the acceptance $A = 0.44$, consistent with the horizontal ($\Delta\theta = \pm 500\,\mathrm{mrad}$) and vertical ($\Delta\phi = \pm 300\,\mathrm{mrad}$) acceptances of the spectrometer scheme describe in Sec. 3.2.

Assuming for 20 useful hours per day of data taking, one gets about 200 events/ day, that is in two periods of 100 days, 40000 dimuons events in the continuum with masses larger than 4 GeV. Such a statistics, remembering the M dependence of the cross-section that decreases by about two order of magnitude from $M = 4\,\mathrm{GeV}$ to $M = 9\,\mathrm{GeV}$, will allow to inspect the $x \to 1$ region where higher twist contributions are expected [41].

For the reaction $\bar{p} + p \to \bar{\Lambda} + \Lambda + X$ a cross-section $\sigma = 400\,\mu\mathrm{b}$ is given [42]. Assuming an acceptance $A = 0.02$, that accounts for the detection of the Λ ($\bar{\Lambda}$) through their weak decay $\Lambda \to p\pi^-$ ($\bar{\Lambda} \to \bar{p}\pi^+$), the expected counting rate is:

$$\boldsymbol{\mathcal{R}} = 2.25 \cdot 10^{31} \times 4 \cdot 10^{-28} \times A = 9.0 \cdot 10^{3} \times A \approx 2 \cdot 10^{2}\,\mathrm{ev.\,s^{-1}} \qquad (15)$$

that means, within the same assumptions as before, $\approx 1.4 \cdot 10^7$ ev/day.

In the case of the open charm production, the cross-section for the $\bar{p}p \to \Lambda_c^+ X$ at 40 GeV is expected to be of the order of the μbarn [43]; the detection of the Λ's coming from the $\Lambda_c^+ \to \Lambda\,\pi^+$ weak decay is affected by the same acceptance as quoted above ($A = 0.02$) and by the branching ratio of the weak decay ($BR_{\Lambda_c^+ \to \Lambda\,\pi^+} = 0.9\,\%$). The expected counting rate is then:

$$\boldsymbol{\mathcal{R}} = 2.25 \cdot 10^{31} \times 1 \cdot 10^{-30} \times 9 \cdot 10^{-3} \times A = 2.02 \cdot 10^{-1} \times A \approx 4 \cdot 10^{3}\,\mathrm{ev.\,s^{-1}} \qquad (16)$$

that means $\approx$ 30000 ev /100 days.

For the proton time like form factors only antiproton beams of energyup to 10 GeV would be selected, because with a luminosity $\boldsymbol{\mathcal{L}} = 2{\cdot}10^{32}$ only 2.4 events/day are expected at $s = 20\,\mathrm{GeV^2}$.

4 Conclusion

The different physics items discussed in Sec. 2 provide excellent tools to deepen the investigation of the nucleonic structure; the ideal tools would be both polarised antiprotons and protons, but even with polarised protons only, plenty of spin effects can be investigated as well.

The key issue is the total energy in the center of mass frame $\sqrt{s}$, in order to allow the investigation of the parton distribution functions in a x Bjorken domain

large enough. This goal can be achieved in two different ways: either with a slow extraction from SIS 300 of an antiproton beam, eventually polarised, of momentum greater than 40 GeV/c, scattering on a fixed polarised target, that can be polarised both transversely and longitudinally; or in an HESR modified to a collider of an antiproton beam, eventually transversely polarised, and of a transversely polarised proton beam.

In the former scenario more information on spin effects could be accessed, since the asymmetries related to both the transverse and the longitudinal polarisation of the nucleon would be investigated.

The latter scenario would have the advantage, for an equal luminosity, of a better factor of merit, for a proton polarisation equal to that of the target, as no dilution factor has to be taken into account in that case. A larger acceptance from the detector point of view could be obtained, being the cut in acceptance for very forward or backward emitted pairs of muons or Λ's smaller. Also the modification to the new GSI facility layout would be smaller (Sec. 3.1).

The collider mode, that is under investigation presently, has evolved in different scenarios, studied to get the highest possible luminosity and including the possibility to use the PANDA detector also for the study of spin physics. In the case of an asymmetric collider, this detector could be used not only for preliminary studies of azimuthal asymmetries for unpolarised protons versus unpolarised antiprotons at the maximum momentum 15 GeV/c, but also to detect single and double spin asymmetries with transversely polarised protons (antiprotons) at $\sqrt{s} \geq 10$ GeV and therefore in a kinematic region where perturbative corrections are expected to be smaller.

References

[1] ASSIA Collaboration: *Letter of Intent for 'A study on Spin-Dependent Interactions with Antiprotons'*, http://www.gsi.de/documents/DOC-2004-Jan-152-1.ps.

[2] Barone, Drago, Ratcliffe: Phys. Rep **359** (2002) 1.

[3] P. L. McGaughey, J. M. Moss and J. C. Peng: Ann. Rev. Nucl. Part. Sci. **49** (1999) 217.

[4] J. Collins and D. E. Soper: Phys. Rev. **D16** (1977) 2219.

[5] E. A. Hawker et al.: Phys. Rev. Lett. **80** (1998) 3715.

[6] M. Anselmino: private communication.

[7] L. P. Gamberg, G. R. Goldstein and K. A. Oganessyan: arXiv:hep-ph/0411220.

[8] PANDA Collaboration: *Letter of Intent for 'Strong Interaction Studies with Antiprotons'*, http://www.gsi.de/documents/DOC-2004-Jan-115-1.pdf.

[9] E. Anassontzis et al.: Phys. Rev.**D38** (1988) 1377.

[10] Barone, Colarco and Drago: Phys. Rev. **D56** (1997) 527.

[11] M. Anselmino et al.: hep-ph/0403114.

[12] D. Boer, S. Brodsky and D. Sung Hwang: Phys. Rev. **D67** (2003) 054003-1.

[13] J. C. Collins: Phys. Lett. **B536** (2002) 43.

[14] Conway et al.: Phys. Rev. **D39** (1989) 22.

[15] D. Boer: Phys. Rev. **D60** (1999) 014012.

[16] A. Bianconi and M. Radici: arXiv:hep-ph/0412368.

[17] N. Hammon, O. Teryaev and A. Schäfer: Phys. Lett. **B390** (1997) 409.

[18] D. Boer, P. J. Mulders and O. Teryaev: Phys. Rev. **D57** (1998) 3057.

[19] D. Boer and P. J. Mulders: Nucl. Phys. **B569** (2000) 505.

[20] D. Boer and J. Qiu: Phys. Rev. **D65** (2002) 034008.

[21] M. Anselmino, U. D'Alesio and F. Murgia: Phys. Rev. **D67** (2003) 074010.

[22] R608 Collaboration, T. Henkes et al.: Phys. Lett. **B283** (1992) 155.

[23] J. Felix et al.: Phys. Rev. Lett. **82** (1999) 5213.

[24] T. A. DeGrand and H. I. Miettinen: Phys. Rev. **D23** (1981) 1227; **D24** (1981) 2419; **D31** (1985) 661(E);
T. A. DeGrand, J. Markkanen, and H. I. Miettinen: Phys. Rev. **D32** (1985) 2445.

[25] B. Andersson, G. Gustafson, and G. Ingelman: Phys. Lett. **B85** (1979) 417.

[26] W. G. D. Dharmaratna and G. R. Goldstein: Phys. Rev. **D41** (1990) 1731;
J. Szwed: Phys. Lett. **B105** (1981) 403.

[27] M. Anselmino, D. Boer, U. D'Alesio and F. Murgia: Phys. Rev. **D63** (2001) 054029.

[28] DISTO Collaboration, F. Balestra et al.: Phys. Rev. Lett. **83** (1999) 1534.

[29] B. E. Bonner et al.: Phys. Rev. Lett. **58** (1987) 447.

[30] A. Bravar et al.: Phys. Rev. Lett. **78** (1997) 4003.

[31] M. A. Alberg, J. Ellis and D. Kharzeev: Phys. Lett. **B365** (1995) 113.

[32] N. K. Pak and M. P. Rekalo: Phys. Lett. **B450** (1999) 443.

[33] K. D. Paschke and B. Quinn: Phys. Lett. **B495** (2000) 49.

[34] PS185 Collaboration, K. D. Paschke et al.: Nucl. Phys. **A692** (2001) 55.

[35] D. L. Adams et al.: Phys. Lett. **B264** (1991) 462;
A. Bravar et al.: Phys. Rev. Lett. **77** (1996) 2626.

[36] J. Adams et al.: e-Print Archive: hep-ex/0310058.

[37] M. Anselmino et al.: Phys. Rev. **D71** (2005) 014002.

[38] S. J. Brodsky: private communication.

[39] The COMPASS Collaboration CERN/SPLC 96-14.

[40] H. Gutbrod: private communication.

[41] S. J. Brodsky, E. L. Berger and G. P. Lepage QCD161:D71:1982 and SLAC-PUB-3027.

[42] R. Baldini et al.: Landolt-Bornstein New Series 1/12b p. 209.

[43] J. Smith and R. Vogt: Z. Phys. **C75** (1997) 271.